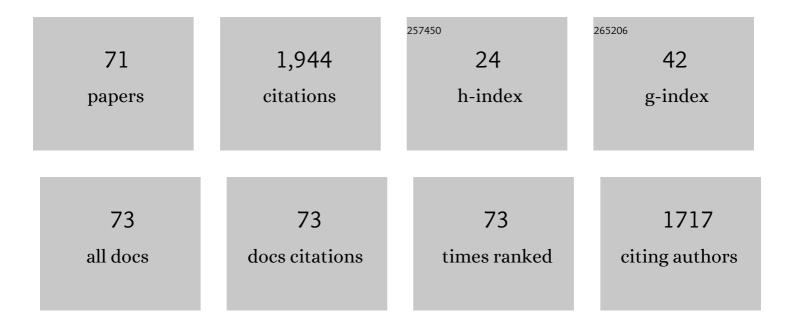
Stephen A Hall

List of Publications by Year in descending order

Source: https://exaly.com/author-pdf/4900651/publications.pdf Version: 2024-02-01



STEDHEN A HALL

#	Article	IF	CITATIONS
1	Grain-scale experimental investigation of localised deformation in sand: a discrete particle tracking approach. Acta Geotechnica, 2012, 7, 1-13.	5.7	276
2	Experimental micro-mechanics of granular media studied by x-ray tomography: recent results and challenges. Geotechnique Letters, 2013, 3, 142-146.	1.2	125
3	Quantifying Interparticle Forces and Heterogeneity in 3D Granular Materials. Physical Review Letters, 2016, 117, 098005.	7.8	109
4	Characterization of shear and compaction bands in a porous sandstone deformed under triaxial compression. Tectonophysics, 2011, 503, 8-17.	2.2	105
5	Localised deformation patterning in 2D granular materials revealed by digital image correlation. Granular Matter, 2010, 12, 1-14.	2.2	101
6	TomoWarp2: A local digital volume correlation code. SoftwareX, 2017, 6, 267-270.	2.6	76
7	Experimental micromechanics: grain-scale observation of sand deformation. Geotechnique Letters, 2012, 2, 107-112.	1.2	75
8	Characterization of pore structure and strain localization in Majella limestone by X-ray computed tomography and digital image correlation. Geophysical Journal International, 2015, 200, 701-719.	2.4	56
9	Can intergranular force transmission be identified in sand?. Granular Matter, 2011, 13, 251-254.	2.2	51
10	Stabilizing nanocellulose-nonionic surfactant composite foams by delayed Ca-induced gelation. Journal of Colloid and Interface Science, 2016, 472, 44-51.	9.4	47
11	Investigating the Onset of Strain Localization Within Anisotropic Shale Using Digital Volume Correlation of Timeâ€Resolved Xâ€Ray Microtomography Images. Journal of Geophysical Research: Solid Earth, 2018, 123, 7509-7528.	3.4	42
12	Characterization of the bone-metal implant interface by Digital Volume Correlation of in-situ loading using neutron tomography. Journal of the Mechanical Behavior of Biomedical Materials, 2017, 75, 271-278.	3.1	41
13	Characterization of fluid flow in a shear band in porous rock using neutron radiography. Geophysical Research Letters, 2013, 40, 2613-2618.	4.0	38
14	Shear-enhanced compaction band identification at the laboratory scale using acoustic and full-field methods. International Journal of Rock Mechanics and Minings Sciences, 2014, 67, 240-252.	5.8	38
15	Scanning 3DXRD Measurement of Grain Growth, Stress, and Formation of Cu6Sn5 around a Tin Whisker during Heat Treatment. Materials, 2019, 12, 446.	2.9	38
16	Localized deformation in intensely fissured clays studied by 2D digital image correlation. Acta Geotechnica, 2013, 8, 247-263.	5.7	36
17	Time-of-Flight Three Dimensional Neutron Diffraction in Transmission Mode for Mapping Crystal Grain Structures. Scientific Reports, 2017, 7, 9561.	3.3	36
18	Reconstructing intragranular strain fields in polycrystalline materials from scanning 3DXRD data. Journal of Applied Crystallography, 2020, 53, 314-325.	4.5	36

STEPHEN A HALL

#	Article	IF	CITATIONS
19	3D-printed monolithic biofilters based on a polylactic acid (PLA) – hydroxyapatite (HAp) composite for heavy metal removal from an aqueous medium. RSC Advances, 2021, 11, 32408-32418.	3.6	35
20	Nanostructurally Controllable Strong Wood Aerogel toward Efficient Thermal Insulation. ACS Applied Materials & Interfaces, 2022, 14, 24697-24707.	8.0	34
21	Strain fields and mechanical response of a highly to medium fissured bentonite clay. International Journal for Numerical and Analytical Methods in Geomechanics, 2013, 37, 1510-1534.	3.3	30
22	Coupled diffusion-deformation multiphase field model for elastoplastic materials applied to the growth of Cu6Sn5. Acta Materialia, 2016, 108, 98-109.	7.9	30
23	Neutron tomographic imaging of bone-implant interface: Comparison with X-ray tomography. Bone, 2017, 103, 295-301.	2.9	29
24	Linking multiscale deformation to microstructure in cortical bone using in situ loading, digital image correlation and synchrotron X-ray scattering. Acta Biomaterialia, 2018, 69, 323-331.	8.3	29
25	Sub-trabecular strain evolution in human trabecular bone. Scientific Reports, 2020, 10, 13788.	3.3	27
26	Experimental characterisation of (localised) Deformation Phenomena in Granular Geomaterials from Sample Down to Inter-and Intra-grain Scales. Procedia IUTAM, 2012, 4, 54-65.	1.2	24
27	Fast 4â€D Imaging of Fluid Flow in Rock by Highâ€&peed Neutron Tomography. Journal of Geophysical Research: Solid Earth, 2019, 124, 3557-3569.	3.4	24
28	An extension of digital volume correlation for multimodality image registration. Measurement Science and Technology, 2017, 28, 095401.	2.6	23
29	Multi-scale mechanics of granular solids from grain-resolved X-ray measurements. Proceedings of the Royal Society A: Mathematical, Physical and Engineering Sciences, 2017, 473, 20170491.	2.1	21
30	Evidence of 3D strain gradients associated with tin whisker growth. Scripta Materialia, 2018, 144, 1-4.	5.2	21
31	Investigating the Mechanical Characteristics of Bone-Metal Implant Interface Using in situ Synchrotron Tomographic Imaging. Frontiers in Bioengineering and Biotechnology, 2018, 6, 208.	4.1	20
32	Three-dimensional experimental granular mechanics. Geotechnique Letters, 2015, 5, 236-242.	1.2	17
33	Bone Damage Evolution Around Integrated Metal Screws Using X-Ray Tomography — in situ Pullout and Digital Volume Correlation. Frontiers in Bioengineering and Biotechnology, 2020, 8, 934.	4.1	16
34	Innovatively processed quinoa (<i>Chenopodium quinoa</i> <scp>W</scp> illd.) food: chemistry, structure and endâ€use characteristics. Journal of the Science of Food and Agriculture, 2022, 102, 5065-5076.	3.5	15
35	Multi-scale Measurement of (Amorphous) Polymer Deformation: Simultaneous X-ray Scattering, Digital Image Correlation and In-situ Loading. Experimental Mechanics, 2014, 54, 1373-1383.	2.0	14
36	Exploring the visual world of fossilized and modern fungus gnat eyes (Diptera: Keroplatidae) with X-ray microtomography. Journal of the Royal Society Interface, 2020, 17, 20190750.	3.4	14

STEPHEN A HALL

#	Article	IF	CITATIONS
37	The Brittleâ€Ductile Transition in Porous Limestone: Failure Mode, Constitutive Modeling of Inelastic Deformation and Strain Localization. Journal of Geophysical Research: Solid Earth, 2021, 126, e2020JB021602.	3.4	14
38	Surface analysis of tissue paper using laser scanning confocal microscopy and micro-computed topography. Cellulose, 2020, 27, 8989-9003.	4.9	12
39	Micro/nano-structural evolution in spruce wood during soda pulping. Holzforschung, 2021, 75, 754-764.	1.9	11
40	Long term evolution of microstructure and stress around tin whiskers investigated using scanning Laue microdiffraction. Acta Materialia, 2019, 168, 210-221.	7.9	10
41	Quantifying local rearrangements in three-dimensional granular materials: Rearrangement measures, correlations, and relationship to stresses. Physical Review E, 2022, 105, 014904.	2.1	10
42	Monitoring of the nano-structure response of natural clay under mechanical perturbation using small angle X-ray scattering and digital image correlation. Acta Geotechnica, 2019, 14, 1965-1975.	5.7	9
43	Combining spectral induced polarization with X-ray tomography to investigate the importance of DNAPL geometry in sand samples. Geophysics, 2019, 84, E173-E188.	2.6	9
44	Dual modality neutron and x-ray tomography for enhanced image analysis of the bone-metal interface. Physics in Medicine and Biology, 2021, 66, 135016.	3.0	9
45	Fast Tracking of Fluid Invasion Using Time-Resolved Neutron Tomography. Transport in Porous Media, 2018, 124, 117-135.	2.6	7
46	3D Strain Field Evolution and Failure Mechanisms in Anisotropic Paperboard. Experimental Mechanics, 2021, 61, 581-608.	2.0	7
47	Fibre directions at a branch-stem junction in Norway spruce: a microscale investigation using X-ray computed tomography. Wood Science and Technology, 2022, 56, 147-169.	3.2	7
48	Innovative Green Way to Design Biobased Electrospun Fibers from Wheat Gluten and These Fibers' Potential as Absorbents of Biofluids. ACS Environmental Au, 2022, 2, 232-241.	7.0	7
49	Prolonged heat and drought versus cool climate on the Swedish spring wheat breeding lines: Impact on the gluten protein quality and grain microstructure. Food and Energy Security, 2022, 11, .	4.3	7
50	Quantifying the hierarchy of structural and mechanical length scales in granular systems. Extreme Mechanics Letters, 2022, 51, 101590.	4.1	6
51	Timelapse ultrasonic tomography for measuring damage localization in geomechanics laboratory tests. Journal of the Acoustical Society of America, 2015, 137, 1389-1400.	1.1	5
52	Localised strain in fissured clays: the combined effect of fissure orientation and confining pressure. Acta Geotechnica, 2022, 17, 1585-1603.	5.7	5
53	Experimental quantification of 3D deformations in sensitive clay during stress-probing. Geotechnique, 2023, 73, 655-666.	4.0	5
54	Microscale deformation mechanisms in paperboard during continuous tensile loading and 4D synchrotron Xâ€ray tomography. Strain, 2022, 58, .	2.4	5

STEPHEN A HALL

#	Article	IF	CITATIONS
55	An alternative method for calibration of flow field flow fractionation channels for hydrodynamic radius determination: The nanoemulsion method (featuring multi angle light scattering). Journal of Chromatography A, 2018, 1533, 155-163.	3.7	4
56	Lupin Protein Isolate Structure Diversity in Frozen-Cast Foams: Effects of Transglutaminases and Edible Fats. Molecules, 2021, 26, 1717.	3.8	4
57	The scale of a martian hydrothermal system explored using combined neutron and x-ray tomography. Science Advances, 2022, 8, eabn3044.	10.3	4
58	The Hydration State of Bone Tissue Affects Contrast in Neutron Tomographic Images. Frontiers in Bioengineering and Biotechnology, 0, 10, .	4.1	4
59	New Remains of Scandiavis mikkelseni Inform Avian Phylogenetic Relationships and Brain Evolution. Diversity, 2021, 13, 651.	1.7	3
60	Impact of Compression on the Electrochemical Performance of the Sulfur/Carbon Composite Electrode in Lithiumâ \in Sulfur Batteries. Batteries and Supercaps, 2022, 5, .	4.7	3
61	Characterisation of Single-Phase Fluid-Flow Heterogeneity Due to Localised Deformation in a Porous Rock Using Rapid Neutron Tomography. Journal of Imaging, 2021, 7, 275.	3.0	3
62	Force measurements in stiff, 3D, opaque granular materials. EPJ Web of Conferences, 2017, 140, 02006.	0.3	2
63	Micromechanics of Granular Media Characterised Using X-Ray Tomography and 3DXRD. Trends in Mathematics, 2018, , 169-176.	0.1	2
64	Analysis of Failure Modes in Fiber Reinforced Concrete Using X-ray Tomography and Digital Volume Correlation. Proceedings (mdpi), 2018, 2, 401.	0.2	2
65	Influence of fissure inclination and confining pressure on the local behaviour of natural clays. E3S Web of Conferences, 2019, 92, 03004.	0.5	2
66	A Continuity Flow Based Tomographic Reconstruction Algorithm for 4D Multi-Beam High Temporal—Low Angular Sampling. Journal of Imaging, 2021, 7, 246.	3.0	2
67	Unravelling the deformation process of a compacted paper: in-situ tensile loading, 4D X-ray tomography and image-based analysis. International Journal of Solids and Structures, 2022, 242, 111539.	2.7	2
68	3D Xâ€Ray Diffraction Characterization of Grain Growth and Recrystallization in Rolled Braze Clad Aluminum Sheet. Advanced Engineering Materials, 2021, 23, 2100126.	3.5	1
69	Characterisation of Grains and Flour Fractions from Field Grown Transgenic Oil-Accumulating Wheat Expressing Oat WRI1. Plants, 2022, 11, 889.	3.5	1
70	<i>In situ</i> microstructural evolution of spruce wood during soda pulping using synchrotron X-ray tomography. Holzforschung, 2022, 76, 611-621.	1.9	1
71	A Bibliometric Study on Swedish Neutron Users for the Period 2006–2020. Neutron News, 2021, 32, 28-33.	0.2	0